

DIRECT PHOTON AND NEUTRAL MESONS MEASUREMENTS WITH THE ALICE DETECTOR*

ADAM MATYJA

on behalf of the ALICE Collaboration

The Henryk Niewodniczański Institute of Nuclear Physics
Polish Academy of Sciences
Radzikowskiego 152, 31-342 Kraków, Poland

(Received May 4, 2016)

The ALICE experiment at LHC is dedicated to studies of the Quark–Gluon Plasma (QGP) state, which is going to be created in heavy-ion collisions. Both photons and neutral mesons are excellent probes for QGP formation. Photons are produced during the different stages of the expansion of the initial hot matter fireball. They do not interact strongly with the medium and passing through it, they carry information on their emission point. The prompt photons which are formed at the early stage of the collision enable us to test perturbative QCD constraining parton distributions and fragmentation functions. Looking into the regime of thermal photons, one can extract the temperature of the medium. The medium-induced energy loss of particles can be investigated via the measurement of neutral meson spectra for different centrality classes as well as via neutral meson–hadron correlations. A decrease of the nuclear modification factor (R_{AA}) with centrality of the collision is observed. The suppression of the away side of the per-trigger yield modification factor (I_{AA}) shows in a similar way the evidence for energy loss in medium. Both direct photons and neutral mesons have been measured by the ALICE experiment. Photons are measured in ALICE directly in the two electromagnetic calorimeters (PHOS and EMCal), as well as via method of photon conversion (PCM) into electron–positron pairs in the inner tracking system (ITS) and the time projection chamber (TPC). Neutral mesons are combined from photon pairs via the invariant mass technique. Results obtained in EMCal, PHOS and PCM are consistent one to the other and allow to measure the spectra of particles with high precision over a wide kinematical range. An overview of the recent results on photon and meson physics from ALICE will be shown.

DOI:10.5506/APhysPolB.47.1529

* Presented at the Cracow Epiphany Conference on the Physics in LHC Run 2, Kraków, Poland, January 7–9, 2016.

1. Introduction

Neutral mesons such as π^0 or η are produced via parton fragmentation in pp collisions. Studies of the hadron production in binary collisions give information about parton distribution functions (PDF) and fragmentation functions (FF). The comparison of meson production between pp and heavy-ion collisions (HIC) allows to observe modification of PDF or FF via linear and non-linear recombination effects caused by the dense matter [1]. The effects visible in the inclusive spectra can be quantified with particle ratio comparison between HIC and pp collisions. Different regimes of transverse momentum spectra provide information about different effects. The bulk properties and collective effects can be studied at low p_T range ($p_T < 3\text{--}5$ GeV/ c). The gluon fragmentation contributes most to π^0 and η meson production at LHC energies. Gluons will suffer a larger energy loss in the medium than quarks due to the different color factor in a gluon–gluon and a quark–gluon vertex. This fact together with a different relative contribution of quarks and gluons to the light meson production may lead to differences in the suppression pattern of π^0 and η mesons [2, 3]. The light meson production at high p_T ($p_T > 5$ GeV/ c) results from hadronization of partons produced in the hard scattering. Thus, they give information about the energy loss of the scattered parton in the dense medium.

Photons are produced at different stages of the expansion of the initial hot matter fireball in Pb–Pb collisions. They do not interact strongly with the medium and passing through it, they carry information on the properties of the matter at the space-time point of their emission [4]. The direct photons which are formed at the early stage of the collision enable us to test perturbative QCD constraining PDF and FF. They contribute the most to the hard part of the direct photon spectrum. Looking into the regime of thermal photons ($p_T < 4$ GeV/ c), one can extract the temperature of the medium. However, the low p_T part of direct photon spectrum contains contributions from all stages of the space-time evolution of the medium. This makes the interpretation of the measured direct photon spectrum difficult due to the additional factor caused by a blue-shift due to the radial flow [5].

This paper is organized in the following way. The method of photon and neutral mesons reconstruction is described in Section 2. The experimental results concerning π^0 and η meson produced in pp and Pb–Pb collisions are presented in Section 3. Section 4 is dedicated to the π^0 -hadron correlation studies, while direct photon analysis is presented in Section 5. We summarize in the last section.

2. Photon and neutral meson reconstruction

The ALICE detector [6] at the LHC [7] contains several sub-detectors made in a large variety of techniques. Photons can be measured with three complementary methods: the photon conversion method (PCM) and calorimeters (PHOS and EMCal). The photon conversion method is based on the external conversion of photon into e^+e^- pair in the material of the detector. Charged particles created in the conversion (as well as other charged hadrons) are registered in the six layers of the silicon inner tracking system (ITS) and the gaseous time projection chamber (TPC). The small conversion probability ($\sim 8.5\%$) is compensated by the full acceptance in azimuth angle and large acceptance in pseudorapidity $|\eta| < 0.9$. Electromagnetic calorimeters measure the energy deposited by photons in the sensitive material. PHOS is a high granularity detector composed of PbWO_4 crystals, with a small acceptance $|\eta| < 0.13$ and $260^\circ < \varphi < 320^\circ$ but high energy resolution. It is located at a radius ~ 460 cm at the bottom of the ALICE detector. EMCal is situated opposite to the PHOS. It covers 100 degrees in azimuth direction φ . It has ~ 700 cm of length in the longitudinal direction, covering $|\eta| < 0.7$. EMCal is placed 430–440 cm out of the Interaction Point in the radial direction. It is made in the shashlik technology. The π^0 and η meson yields are obtained via the measurement of the invariant mass of the photon pairs, each pair measured with one of the three mentioned methods.

3. Neutral mesons

ALICE has measured π^0 production spectra for four center-of-mass energies $\sqrt{s} = 0.9$ [8], 2.76 [9], 7 [8] and 8 TeV [10] in pp collisions. The spectra were measured by PHOS and PCM except the highest energy result where only PHOS was used. The p_T distributions presented in Fig. 1 are described by PYTHIA 8.176 event generator (tune 4C — dashed and Monash — dash-dotted line). Also p_T spectra are compared to the next-to-leading order perturbative QCD (NLO pQCD) calculations for two (and the same) renormalization and factorization scales ($\mu = 2p_T$ — dotted and $\mu = p_T/2$ — small dashed). The MSTW PDF and DSS14 FF [11] used in predictions describe better the measured spectra than previously used calculations [8]. However, the larger the center-of-mass energy and p_T , the larger discrepancy between pQCD and data is observed. Ratio data to prediction/fit for different energies are shown in the four bottom panels of Fig. 1.

Results for six centrality classes in Pb–Pb collisions at $\sqrt{s_{NN}} = 2.76$ TeV [9] are presented in the left panel of Fig. 2. Data are described there by Tsallis and a power law fit. The comparison of π^0 spectra in Pb–Pb collisions with predictions of EPOS event generator [13] and Nemchik *et al.* calcula-

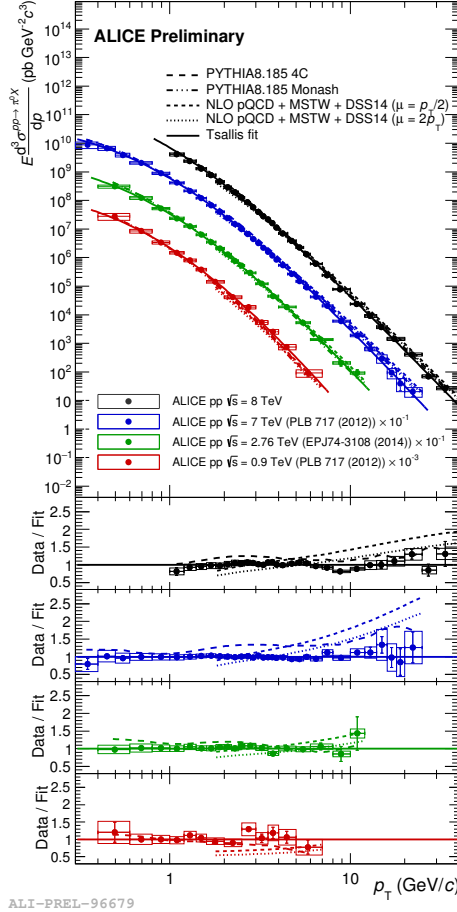


Fig. 1. π^0 production spectra in pp collisions for energies $\sqrt{s} = 0.9, 2.76, 7$ and 8 TeV compared to PYTHIA, NLO pQCD calculations and described by Tsallis fit.

tions [14] for three centrality classes is shown in the right panel of Fig. 2. Both predictions show different degree of agreement with experimental measurements.

Nuclear effects are quantified via the nuclear modification factor R_{AA} defined as: $R_{AA}(p_T) = \frac{1}{N_{\text{coll}}} \frac{dN_{AA}/dp_T}{dN_{pp}/dp_T}$, where dN/dp_T is the yield in nuclear and pp collisions scaled by the number of binary nucleon–nucleon collisions, N_{coll} , obtained from Glauber Monte Carlo simulations [15]. The interplay of the initial (Cronin, nuclear shadowing) and the final (collisional and radiative energy loss) state effects contribute to the nuclear modification factor. There is no impact of medium when $R_{AA} = 1$. Left panel of Fig. 3 shows the p_T dependence of R_{AA} for three centrality classes [9]. The largest sup-

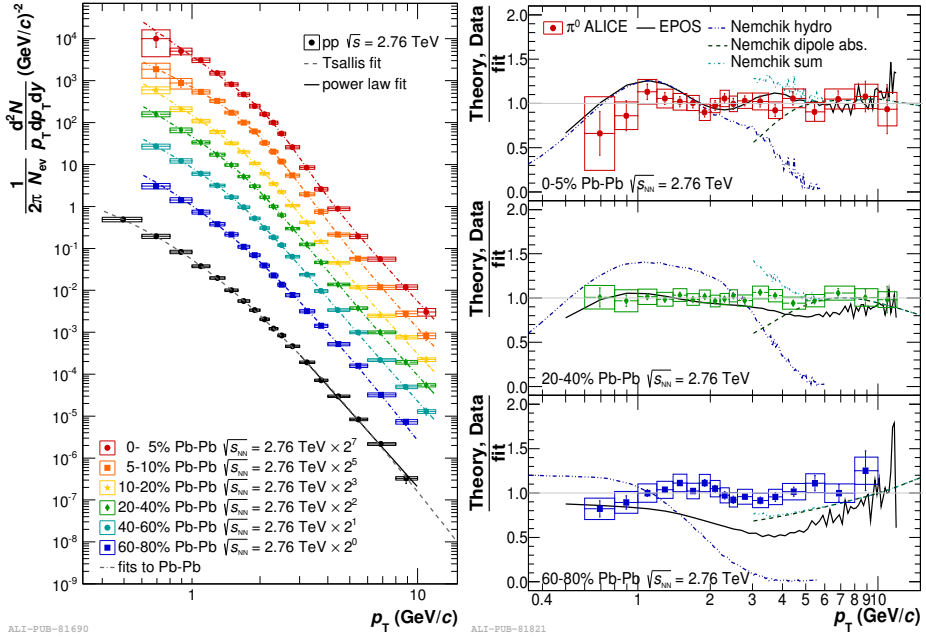


Fig. 2. Left: π^0 yields in Pb–Pb and pp collisions at $\sqrt{s_{NN}} = 2.76$ TeV together with power law and Tsallis fits [9]. Right: Comparison of π^0 spectra in Pb–Pb collisions with predictions of EPOS event generator and Nemchik *et al.* calculations (for different components) for three centrality classes [9].

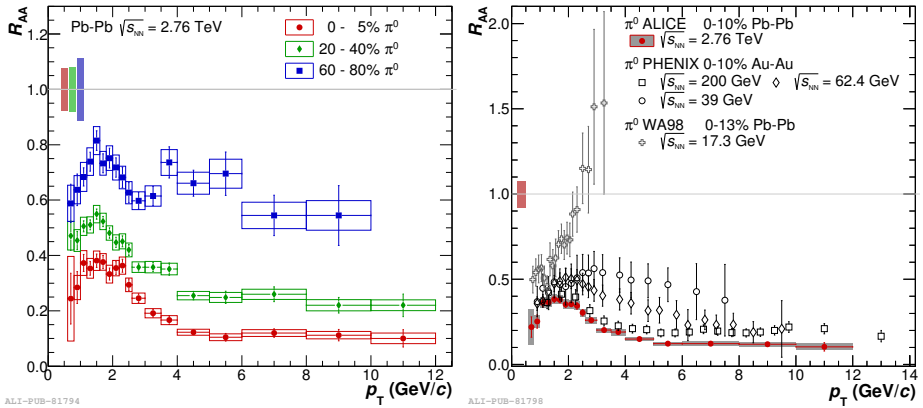


Fig. 3. Left: Neutral pion nuclear modification factor R_{AA} for three centrality classes in Pb–Pb collisions at $\sqrt{s_{NN}} = 2.76$ TeV [9]. Right: Comparison of neutral pion nuclear modification factor R_{AA} in Pb–Pb collisions at $\sqrt{s_{NN}} = 2.76$ TeV for 0–10% centrality class [9] to the lower energy results at RHIC and SPS [16].

pression is observed for the most central Pb–Pb collisions with a value of $R_{AA} \sim 0.1$ above $p_T \approx 4$ GeV/ c . The comparison of the ALICE measurement with other experiments [9, 16] at lower $\sqrt{s_{NN}}$ is shown in the right panel of Fig. 3. A similar modification shape is visible for the two highest center-of-mass energies per nucleon pair. The ALICE result shows a larger suppression than the top energy RHIC result although spectra are flatter in the case of ALICE. The onset of the suppression starts between $\sqrt{s_{NN}} = 17.3$ GeV and $\sqrt{s_{NN}} = 39$ GeV.

The increase of the integrated luminosity up to $L \sim 0.1$ nb $^{-1}$ (10 times more statistics with respect to the previous ALICE result [9]) allowed to extend the p_T range of π^0 spectrum in Pb–Pb collisions at $\sqrt{s_{NN}} = 2.76$ TeV up to 20 GeV/ c . The corresponding π^0 spectra as well as the first existing heavy-ion measurement at the LHC of p_T spectra of the η meson [10] for two centrality classes are shown in the left and right panel of Fig. 4, respectively. These results, which were measured with EMCAL and PCM, are compared to NLO pQCD predictions [11] in pp collisions scaled by N_{coll} . We observe a significant discrepancy in theory NLO pQCD calculations with respect to our measurement.

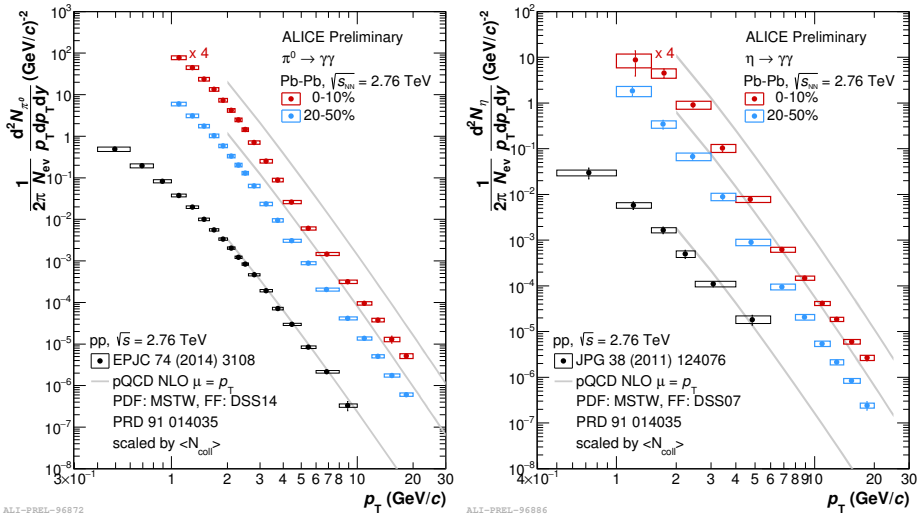


Fig. 4. Invariant differential yield of π^0 (left) and η meson (right) in Pb–Pb collisions at $\sqrt{s_{NN}} = 2.76$ TeV for two centrality classes compared to pp data and NLO pQCD predictions scaled by N_{coll} .

The measured η/π^0 production ratios in Pb–Pb collisions for two centrality classes shown in Fig. 5 are compared to the pp result at $\sqrt{s} = 7$ TeV [8], a theory prediction based on NLO and jet quenching [2] and K^\pm/π^\pm result [17] at the same collision energy and centrality. The η/π^0 ratio is flat

above $p_T = 4$ GeV/ c . The obtained results indicate no significant differences in the ratio for pp and Pb–Pb collisions and agreement with pQCD predictions within uncertainties. Moreover, no impact of strange quark content is visible when compared K^\pm/π^\pm and η/π^0 ratios. The large uncertainties on the η/π^0 ratio in Pb–Pb collisions do not allow us to make any statement on comparison to the corresponding pp result or Pb–Pb result for the K^\pm/π^\pm ratio.

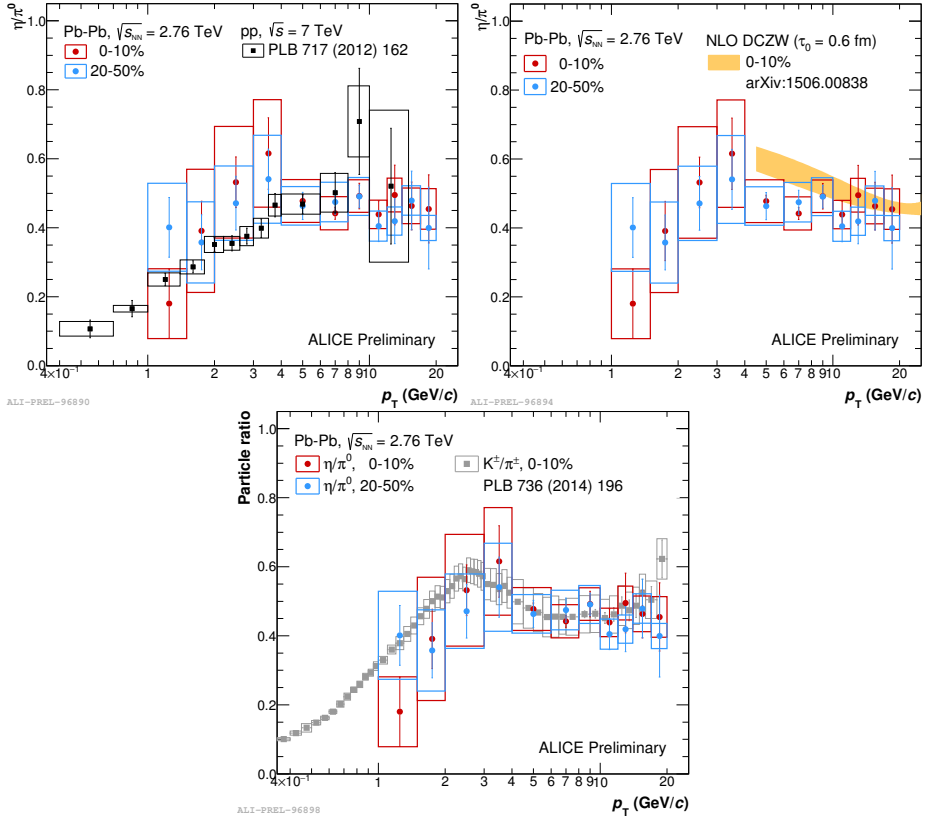


Fig. 5. The η to π^0 meson production ratio in Pb–Pb collisions at $\sqrt{s_{NN}} = 2.76$ TeV for two centrality classes compared to pp result at $\sqrt{s} = 7$ TeV (top left), NLO theoretical calculation with quenching (top right), and K^\pm/π^\pm ratio in central Pb–Pb collisions at $\sqrt{s_{NN}} = 2.76$ TeV (bottom).

4. π^0 -hadron correlations

A parton scattered in the initial stages of the heavy-ion collision goes through the medium. It may lose a fraction of the energy and fragments into many hadrons out of the medium. High p_T hadrons are likely issued

by the fragmentation of partons produced close to the medium surface that traverse a short length in the medium, while low p_T hadrons usually emerge from a parton traversing the maximum length. Two particle correlations analysis provides us information on the amount and distribution of the parton energy loss in the medium via the measurement of the hadrons produced in the parton fragmentation (jets). To quantify this effect, one can look into the azimuthal correlation $\Delta\varphi = \varphi^{\text{trig}} - \varphi^{\text{assoc}}$ of high p_T trigger particle of azimuth φ^{trig} and associated particle of azimuth φ^{assoc} . The correlations between π^0 mesons and charged hadrons in pp collisions at $\sqrt{s} = 2.76$ TeV are presented in Fig. 6 for a given range of trigger particle transverse momentum p_T^{trig} and several ranges of associated particle transverse momentum p_T^{assoc} . The triggered π^0 has been measured with the EMCal and associated charged hadrons have been measured with ITS and TPC. There are two

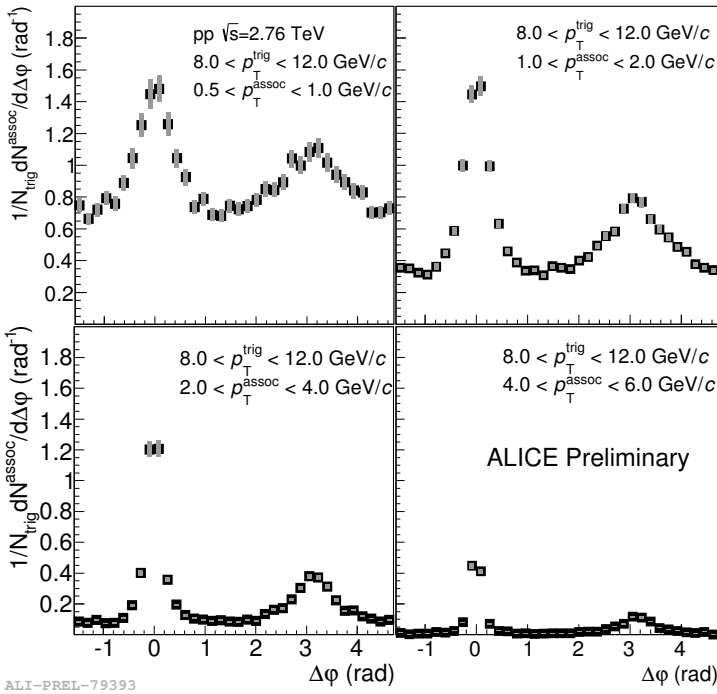


Fig. 6. Azimuthal correlation between π^0 meson and charged hadron in pp collisions at $\sqrt{s} = 2.76$ TeV for π^0 transverse momentum $8 < p_T^{\text{trig}} < 12$ GeV/ c in several p_T^{assoc} ranges.

well-defined structures on each histogram in Fig. 6. The near-side peak is located close to $\Delta\varphi = 0$ while on the opposite azimuthal direction of the trigger particle ($\Delta\varphi = \pi$) the away-side peak appears. Figure 7 illustrates the same azimuthal correlation but for HIC at $\sqrt{s_{NN}} = 2.76$ TeV. The large

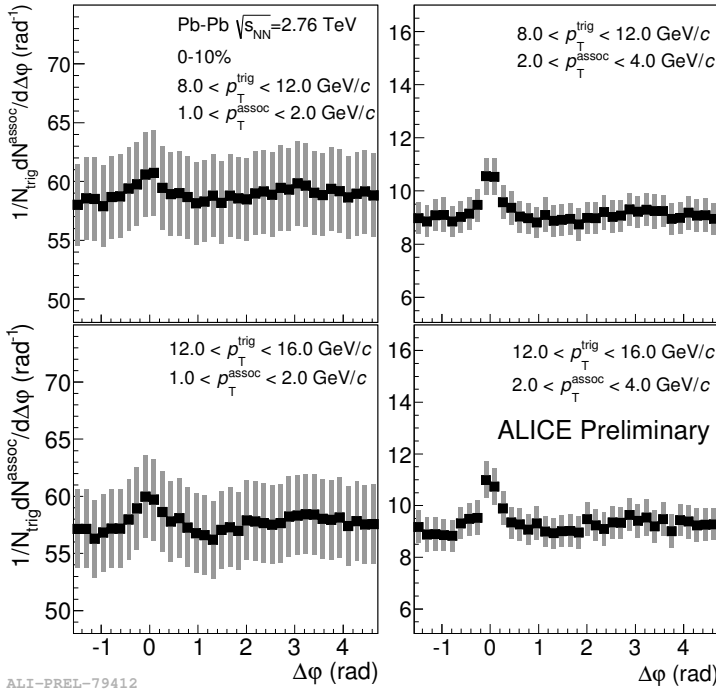


Fig. 7. Azimuthal correlation between π^0 meson and charged hadron in Pb–Pb collisions at $\sqrt{s_{NN}} = 2.76$ TeV for different π^0 transverse momenta p_T^{trig} and two associated particle transverse momentum ranges p_T^{assoc} . Combinatorial background under the peak is not subtracted.

combinatorial background makes both peaks barely visible. The observable which can quantify the effect of the suppression is the medium induced per-trigger yield modification factor $I_{AA}(p_T^{\pi^0}, p_T^{h^\pm}) = \frac{Y^{AA}(p_T^{\pi^0}, p_T^{h^\pm})}{Y^{pp}(p_T^{\pi^0}, p_T^{h^\pm})}$, where $Y^{AA}(p_T^{\pi^0}, p_T^{h^\pm})$ is the per-trigger yield for given trigger particle $p_T^{\pi^0}$ and the associated particle $p_T^{h^\pm}$. The ZYAM (zero yield at minimum) method of the combinatorial background subtraction is used to extract correlated yield of charged hadrons. The per-trigger yield modification factor for the near side and the away side are shown in the left and the right side of Fig. 8, respectively. Our results indicate an enhancement on the near side ($I_{AA} \approx 1.2$), probably due to the modification of the fragmentation function, quark jet to gluon jet ratio modification or bias in the parton p_T due to the energy loss. A suppression is observed on the away side ($I_{AA} \approx 0.6$), which is a manifestation of the energy loss in medium. The I_{AA} results for the π^0 -hadron correlation are in a good agreement with the charged di-hadron correlation measurements in ALICE [18].

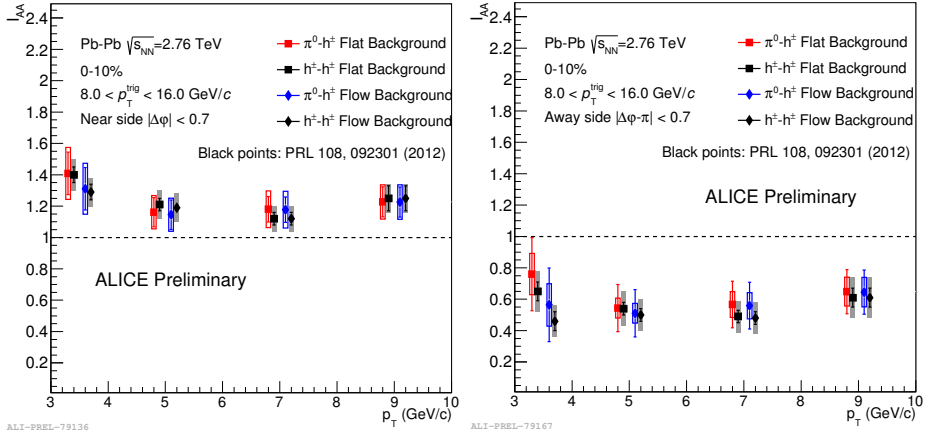


Fig. 8. Per-trigger yield ratio for the near side (left) and the away side (right) for π^0 -hadron correlations compared to h^\pm - h^\pm correlation results.

5. Direct photons

To extract a direct photon (γ_{direct}) signal from data, the inclusive photon (γ_{inc}) spectra have been measured at first. Then, decay photon (γ_{decay}) spectra have been calculated using either measured data or m_T scaling for the unmeasured sources. The main source of decay photons comes from π^0 and η meson decays ($\sim 80\%$ and $\sim 10\text{--}12\%$, respectively). The direct photon spectra have been extracted via a statistical subtraction method: $\gamma_{\text{direct}} = \gamma_{\text{inc}} - \gamma_{\text{decay}} = (1 - \frac{\gamma_{\text{decay}}}{\gamma_{\text{inc}}})\gamma_{\text{inc}} = (1 - \frac{1}{R})\gamma_{\text{inc}}$, where $R = \gamma_{\text{inc}}/\gamma_{\text{decay}}$. In order to reduce some uncertainties, a double ratio $R_\gamma = \frac{\gamma_{\text{inc}}}{\pi_{\text{param}}^0} / \frac{\gamma_{\text{decay}}}{\pi_{\text{cocktail}}^0} \approx R$ was introduced. π_{param}^0 stands here for the parameterized measured π^0 spectrum and π_{cocktail}^0 is the π^0 spectrum evaluated from Monte Carlo. A value of the double ratio R_γ greater than one indicates a presence of direct photons.

The double ratio for pp collisions at $\sqrt{s} = 7$ TeV measured with PCM is shown in Fig. 9. The result is consistent with no signal and the theoretical prediction is within the uncertainties of the measurement. R_γ for three centrality classes in Pb-Pb collisions at $\sqrt{s_{NN}} = 2.76$ TeV measured with PCM and PHOS is shown in the left panel of Fig. 10 [19]. The clear excess visible for all centrality classes in high p_T region is compatible with N_{coll} scaled NLO pQCD predictions and JETPHOX generator with different PDF and FF. However, there remains an excess for the low $p_T < 4$ GeV/c in the most central collisions with a statistical significance of 2.6σ for the region $0.9 < p_T < 2.1$ GeV/c. The direct photon spectra for three centrality classes

are shown in the right panel of Fig. 10. Here, again, a similar excess over N_{coll} scaled NLO pQCD predictions or JETPHOX generator is visible for the low p_T range for the most central and semi-central Pb–Pb collisions.

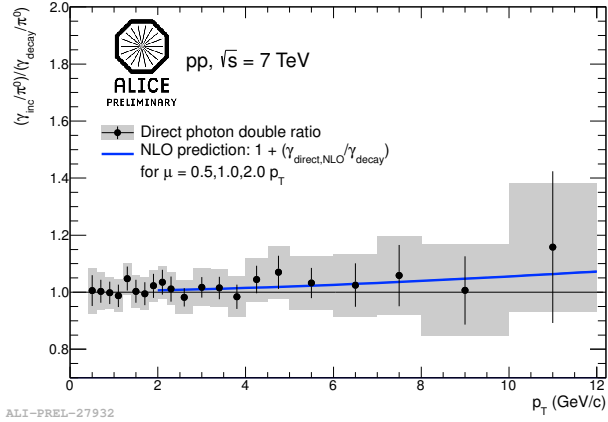


Fig. 9. Double ratio R_γ in pp collisions at $\sqrt{s} = 7$ TeV compared to NLO predictions.

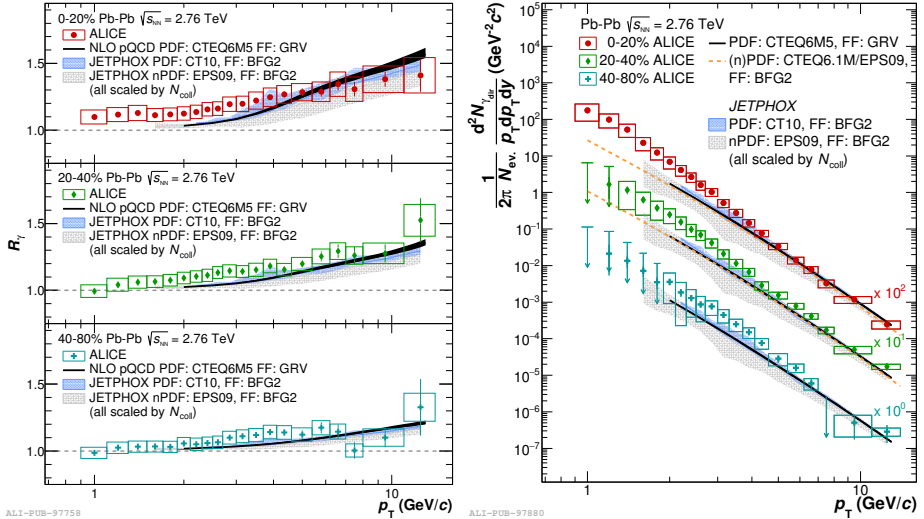


Fig. 10. Double ratio R_γ (left) and direct photon spectra (right) in Pb–Pb collisions at $\sqrt{s_{NN}} = 2.76$ TeV for three centrality classes compared to NLO pQCD predictions and JETPHOX event generator results scaled by N_{coll} [19].

Predictions of various theoretical models [20–23] were compared to the direct photon spectra measured in Pb–Pb collision. This is shown in the left panel of Fig. 11. All models incorporate photons from hard scattering

processes calculated by pQCD and assume QGP formation treated with different assumptions (initial conditions, formation time τ_0 , initial temperature T_{init}). All models describe the data within uncertainties and, currently, it is difficult to distinguish which one suits the data better.

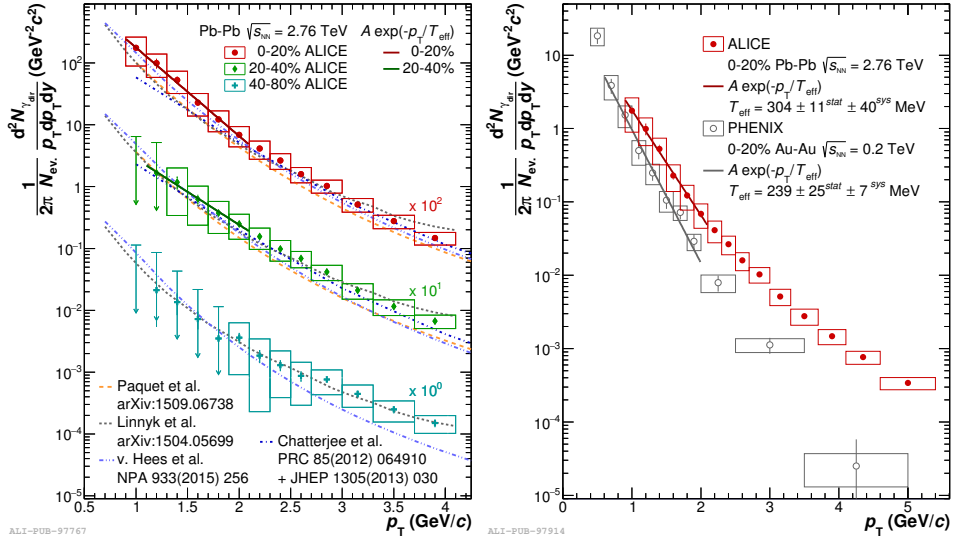


Fig. 11. Left: Direct photon spectra in Pb–Pb collisions at $\sqrt{s_{NN}} = 2.76$ TeV for three centrality classes compared to different theoretical models [19]. Right: The most central Pb–Pb direct gamma spectrum at $\sqrt{s_{NN}} = 2.76$ TeV in ALICE compared to Au–Au PHENIX data at $\sqrt{s_{NN}} = 0.2$ TeV. Exponential fits to both data sets are overlaid.

The direct gamma spectrum for the 0–20% most central Pb–Pb events at $\sqrt{s_{NN}} = 2.76$ TeV in ALICE compared to Au–Au PHENIX data at $\sqrt{s_{NN}} = 0.2$ TeV for the same centrality class [24] is shown in the right panel of Fig. 11. Both spectra were fitted with an exponential function $f(p_T) = A \exp(-p_T/T_{\text{eff}})$ in the range of $0.9 < p_T < 2.2$ GeV/c and $0.6 < p_T < 2$ GeV/c for ALICE and PHENIX data, respectively, to extract the inverse slope parameter T_{eff} . The parameter obtained from the fit to the PHENIX data is $T_{\text{eff}} = 239 \pm 25(\text{stat.}) \pm 7(\text{syst.})$ MeV, while for ALICE is $T_{\text{eff}} = 304 \pm 11(\text{stat.}) \pm 40(\text{syst.})$ MeV, a larger value which translates into a larger initial temperature of the medium for a larger collision energy.

To quantify the effect, the R_{AA} was calculated for direct photons using pQCD calculation from [20] as pp reference. The direct photon R_{AA} for the most central collisions is shown in Fig. 12. The strong enhancement $R_{AA} > 6$ for low p_T range is visible.

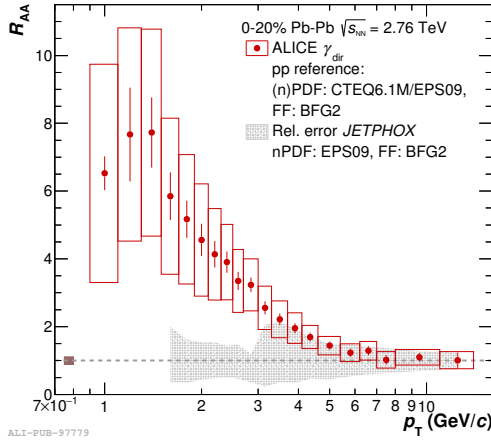


Fig. 12. Nuclear modification factor of direct photons for the most central Pb–Pb collisions at $\sqrt{s_{NN}} = 2.76$ TeV.

6. Summary

In this paper, we presented measurements of the invariant π^0 yields in pp collisions for four center-of-mass energies $\sqrt{s} = 0.9, 2.76, 7$ and 8 TeV as well as for Pb–Pb collisions at $\sqrt{s_{NN}} = 2.76$ TeV in a wide p_T range. The NLO pQCD predictions describe quite well pp results at lower energies, while there is an increasing discrepancy at large p_T for two highest energies. Theoretical models partially describe the π^0 spectra in Pb–Pb collisions. The nuclear modification factor R_{AA} for Pb–Pb collisions at $\sqrt{s_{NN}} = 2.76$ TeV indicates a strong and p_T dependent π^0 suppression. The R_{AA} ALICE result fits well in the overall picture given by other lower center-of-mass energy experiments.

The first η meson measurement at the LHC in HIC has been shown. The η/π^0 ratio shows a complex behavior, rising towards $p_T = 4$ GeV/ c and then remaining essentially flat for higher p_T values. No significant difference has been found between pp and Pb–Pb results as well as when compared to the K^\pm/π^\pm ratio.

The π^0 -hadron correlations have been measured in pp and the most central Pb–Pb collisions. The observed away-side suppression manifests the energy loss in medium.

ALICE has measured direct photon R_γ , spectra and R_{AA} for several centrality classes in Pb–Pb collisions at $\sqrt{s_{NN}} = 2.76$ TeV. The excess over N_{coll} scaled NLO pQCD predictions in low p_T region is visible for each observable. Various models with QGP formation which tried to describe the data show different levels of agreement. The inverse slope parameter obtained from the exponential fit to the most central Pb–Pb events has been found to be $T_{eff} = 304 \pm 11(\text{stat.}) \pm 40(\text{syst.})$ MeV.

I would like to thank the Polish National Science Centre for the supporting grant DEC-2012/05/D/ST2/00855.

REFERENCES

- [1] T. Lappi, H. Mäntysaari, *Phys. Rev. D* **88**, 114020 (2013).
- [2] W. Dai, X.-F. Chen, B.-W. Zhang, E. Wang, *Phys. Lett. B* **750**, 390 (2015).
- [3] X. Guo, X.-N. Wang, *Phys. Rev. Lett.* **85**, 3591 (2000).
- [4] S. Turbide, R. Rapp, C. Gale, *Phys. Rev. C* **69**, 014903 (2004).
- [5] C. Shen, U. Heinz, J.-F. Paquet, C. Gale, *Phys. Rev. C* **89**, 044910 (2014).
- [6] K. Aamodt *et al.* [ALICE Collab.], *JINST* **3**, S08002 (2008).
- [7] L. Evans *et al.*, *JINST* **3**, S08001 (2008).
- [8] B. Abelev *et al.* [ALICE Collab.], *Phys. Lett. B* **717**, 162 (2012).
- [9] B. Abelev *et al.* [ALICE Collab.], *Eur. Phys. J. C* **74**, 3108 (2014).
- [10] A. Morreale [ALICE Collab.], [arXiv:1512.05250](https://arxiv.org/abs/1512.05250) [nucl-ex].
- [11] D. de Florian *et al.*, *Phys. Rev. D* **91**, 014035 (2015).
- [12] A. Adare *et al.* [PHENIX Collab.], *Phys. Rev. C* **88**, 024906 (2013).
- [13] K. Werner *et al.*, *Phys. Rev. C* **85**, 064907 (2012).
- [14] B.Z. Kopeliovich, J. Nemchik, I.K. Potashnikova, I. Schmidt, *Phys. Rev. C* **86**, 054904 (2012).
- [15] M.L. Miller, K. Reygers, S.J. Sanders, P. Steinberg, *Annu. Rev. Nucl. Part. Sci.* **57**, 205 (2007); B. Abelev *et al.* [ALICE Collab.], *Phys. Lett. B* **720**, 52 (2013).
- [16] A. Adare *et al.* [PHENIX Collab.], *Phys. Rev. Lett.* **109**, 152301 (2012); **101**, 232301 (2008); M.M. Aggarwal *et al.* [WA98 Collab.], *Phys. Rev. Lett.* **100**, 242301 (2008).
- [17] B. Abelev *et al.* [ALICE Collab.], *Phys. Lett. B* **736**, 196 (2014).
- [18] K. Aamodt *et al.* [ALICE Collab.], *Phys. Rev. Lett.* **108**, 092301 (2012).
- [19] J. Adam *et al.* [ALICE Collab.], *Phys. Lett. B* **754**, 235 (2016).
- [20] J.-F. Paquet *et al.*, *Phys. Rev. C* **93**, 044906 (2016) [[arXiv:1509.06738](https://arxiv.org/abs/1509.06738) [hep-ph]].
- [21] H. van Hees, M. He, R. Rapp, *Nucl. Phys. A* **933**, 256 (2015).
- [22] R. Chartterjee, H. Holopainen, T. Renk, K.J. Escola, *Phys. Rev. C* **85**, 064910 (2012).
- [23] O. Linnyk, V. Konchakovski, T. Steinert, W. Cassing, *Phys. Rev. C* **92**, 054914 (2015) [[arXiv:1504.05699](https://arxiv.org/abs/1504.05699) [nucl-th]].
- [24] A. Adare *et al.* [PHENIX Collab.], *Phys. Rev. C* **91**, 064904 (2015).